Hg^{2+} detection using phosphorothioate RNA probe adsorbed on graphene oxide and a comparison with thymine-rich DNA

Po-Jung Jimmy Huang, Courtney van Ballegooie, and Juewen Liu*

Department of Chemistry, Waterloo Institute for Nanotechnology

University of Waterloo, Waterloo, Ontario, N2L 3G1, Canada

Fax: 519 7460435; Tel: 519 8884567 Ext. 38919

E-mail: liujw@uwaterloo.ca

Abstract

Mercury is a highly toxic heavy metal and many DNA-based biosensors have been recently developed for Hg^{2+} detection in water. Among them, thymine-rich DNA is the most commonly used for designing Hg^{2+} sensors. However, the thymine-Hg^{2+} interaction is strongly affected by buffer conditions. We recently reported a molecular beacon containing phosphorothioate (PS)-modified RNA linkages that can be cleaved by Hg^{2+}. In this work, the fluorescence quenching and DNA adsorption properties of nano-sized graphene oxide (NGO) were used to develop a new sensor using the PS-RNA chemistry. Three DNA probes were tested, containing one, three and five PS-RNA linkages, respectively. Finally, a fluorophore-labeled poly-A DNA with five PS-RNA linkages was selected and adsorbed by NGO. In the presence of Hg^{2+}, the fluorophore was release from NGO due to the cleavage reaction, resulting in fluorescence enhancement. This sensor is highly selective for Hg^{2+} with a detection limit of 8.5 nM Hg^{2+}. For comparison, a fluorophore-labeled poly-T DNA was also tested, which responded to Hg^{2+} slower and was inhibited by high NaCl concentrations, while the PS-RNA probe was more tolerable to different buffer conditions. This work indicates a new way of interfacing DNA with NGO for Hg^{2+} detection.

Introduction

Mercury is a highly toxic heavy metal.[1] It has now been well documented that even low levels of exposure to mercury cause adverse neurological and somatic health effects, most notably nerve and organ damage.[2] While many analytical instruments are suitable for Hg^{2+} detection, their availability is limited to large centralized labs with a slow turnaround time. One potential alternative solution is the use of biosensors.[3] Biosensors provide on-site and real-time information in a cost-effective manner. One of the most attractive biomolecules for metal detection is DNA.[4-6] DNA has many favorable characteristics, including versatility in metal coordination and inherent high stability; additionally, it is easily modified and programmable.[7-10]

In recent years, a number of DNA-based strategies have been developed to detect Hg^{2+}. The most popular method employs the thymine-Hg^{2+}-thymine interaction, where Hg^{2+} can convert a T-T mismatch to a Hg^{2+}-mediated base pair in a duplex DNA.[11-15] While this interaction is highly specific for Hg^{2+}, it is strongly influenced by buffer conditions such as pH, temperature, ionic strength, and anion species,[16,17] making it difficult for detection in real sample matrix. Another strategy relies on RNA-cleaving DNAzymes.[13,18-20] While many metal ions can directly activate DNAzyme catalysis,[21-23] Hg^{2+} requires the aptazyme technology (i.e. mercury recognition still relies on the above thymine chemistry),[13] or using modified nucleotides.[20] These modified nucleotides, however, are not commercially available, also limiting their analytical applications.

We recently reported a new method by incorporating a phosphorothioate (PS)-modified RNA linkage into a DNA oligonucleotide.[24] Hg^{2+} efficiently cleaves the PS-RNA linkage due to its extremely strong thiophilicity. This method has excellent specificity for Hg^{2+} and the reaction proceeds very quickly. For our initial proof-of-concept, a molecular-beacon-based sensor was

designed, and cleavage of the beacon by Hg^{2+} resulted in fluorescence enhancement. This beacon contained a fluorophore, a quencher and three PS-RNA linkages, making the synthesis expensive with a low yield.[24] Signaling for Hg^{2+} relies on the dissociation of the hairpin, which is strongly affected by salt concentration. Our current objective is to develop a new sensing strategy to overcome these limitations, while maintaining the specificity and sensitivity of the original PS-RNA.

Graphene oxide (GO) is an excellent platform for developing DNA-based fluorescent biosensors.[25-28] Single-stranded DNA is readily adsorbed by GO, and the attached fluorophore is efficiently quenched.[29-31] Addition of a target molecule can recover the fluorescence due to probe desorption.[32] We hypothesize that cleavage of the PS-RNA linkage on GO might also produce a similar signal and, if so, we could eliminate the need for the internal quencher. In this research, we use nano-sized GO (NGO) as a quencher to develop a new sensor based on the PS-RNA chemistry. We also compare the PS-RNA strategy with the commonly used poly-thymine probe in various buffer conditions. This comparison has reinforced an important but commonly neglected aspect of Hg^{2+} sensing: the effect of Cl^-.

Materials and Methods

Chemicals

The fluorophore-labeled DNAs were purchased from Integrated DNA Technologies (IDT, Coralville, IA). GO was purchased from ACS Material, LLC (Medford, MA). The exact DNA sequences used in this study are listed in Figure 1. Cerium chloride heptahydrate, ammonium cerium nitrate, magnesium chloride tetrahydrate, manganese chloride tetrahydrate, cobalt

chloride hexahydrate, nickel chloride, copper chloride dihydrate, zinc chloride, cadmium chloride hydrate, mercury perchlorate, lead acetate, lithium chloride, sodium chloride, rubidium chloride, potassium chloride, calcium chloride dihydrate, cesium chloride, strontium chloride hexahydrate, barium chloride, silver nitrate, yttrium chloride hexahydrate, scandium chloride hydrate, chromium chloride hexahydrate, indium chloride, gallium chloride, aluminum chloride hydrate, thallium chloride, and nickel chloride were purchased from Sigma-Aldrich. Iron (II) chloride tetrahydrate and iron (III) chloride hexahydrate were from Alfa Aesar. The metal solutions were prepared by directly dissolving the salts in Milli-Q water. 2-[4-(2-hydroxyethyl)piperazin-1-yl]-ethanesulfonic acid (HEPES) and sodium chloride were from Mandel Scientific Inc. (Guelph, ON). 4-Morpholinepropanesulfonic acid (MOPS), tetramethylethylenediamine (TEMED), urea, ammonium persulfate (APS), and 40% (w/v) acrylamide–bis-acrylamide (29 : 1) were obtained from Bio Basic Inc. (Markham, ON, Canada).

Fluorescent assay using the PS-RNA probe

NGO was prepared by dispersing the GO sheets in water (0.5 mg/mL) and sonicating with ultrasonic processor (120 W 20 kHz with pulse on for 2 s and pulse off for 4 s for 10 h) at room temperature. The fluorescent of FAM-labeled probes were first quenched by NGO in buffer A (50 mM NaCl, 0.5 mM $MgCl_2$, 50 mM MOPS, pH 7.5). For each assay, 100 μL of sensor probe (20 nM) was mixed with NGO (15 μg/mL) in each well. Sensors were equilibrated at 23 °C for five min before 1 μL of metal ion solution was added. The kinetic studies were carried out in 96 well plates and were monitored continuously for 1 h with a SpectraMax M3 microplate reader (Ex = 490 nm; Em = 520 nm).

Fluorescent assay using the poly-T probe

To understand the potential interference of Cl^- in poly-T DNA-based sensing, buffers containing NaCl or $NaNO_3$ were compared. For each sample, 20 nM of the probe was diluted in buffer B (20 mM MOPS, pH 7.5) in the presence of various concentrations of NaCl or $NaNO_3$. Each well contained 15 μg/mL NGO. For fluorescent kinetic measurement, the same parameters were used as the PS-RNA probe described above.

Gel electrophoresis

For each sample, 0.75 μM probe was incubated with 10 μM metal ions in buffer (25 mM NaCl, 50 mM MOPS, pH 7.5) for 5 min. The reaction was quenched afterward by 1 X gel loading dye containing 11 mM EDTA and 8 M urea. The reaction products were then separated using 15% denaturing polyacrylamide gel (dPAGE) at 200 V for 80 min. Gel images were acquired with a Bio-Rad ChemiDoc MP imaging system.

Results and Discussion

Sensor design principles. Our sensor design is shown in Figure 1A. The DNA probe contains three components: a poly-adenine segment (15 adenines) for adsorption by NGO (adenine is known to have high affinity for GO);[33] one or more PS-RNA linkages serving as the cleavage site(s); and a fluorophore. The fluorophore is positioned nearby the PS-RNA sites so that it can be readily released from NGO after the cleavage reaction. The reason that more than one PS-RNA linkage might be needed is due to the low cleavage yield. Once Hg^{2+} is added, only ~16% of each PS-RNA linkage undergoes cleavage,[24] while the rest are desulfurized to the normal

phosphate backbone and cannot be further cleaved by Hg^{2+}.[34] To optimize the design, we tested DNAs with 1, 3, and 5 PS-RNA linkages (Probe 1-3). The chemistry of the cleavage reaction is shown in Figure 1B.

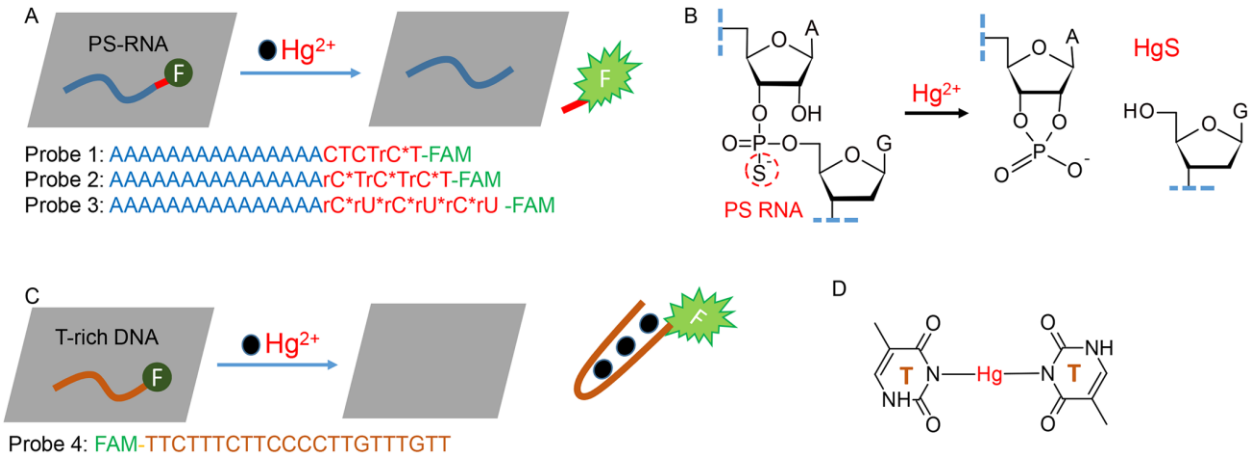

Figure 1. Biosensor designs. (A) The PS-RNA based sensors. A poly-A DNA is used to attach to NGO. Hg^{2+} cleaves the probes and release the fluorophore-labeled fragment to produce fluorescence signal. The DNA sequences are listed from the 5′-end, and the PS linkages are denoted by the asterisks. (B) The Hg^{2+}-induced PS-RNA cleavage reaction. (C) The T-rich DNA based sensor. Hg^{2+} induces probe desorption by forming a hairpin DNA. (D) The structure of the T-Hg^{2+}-T complex.

For comparison, a thymine-rich DNA (Probe 4) is also used (Figure 1C), and it can also be adsorbed by NGO. In the presence of Hg^{2+}, a folded hairpin structure is formed, resulting in DNA desorption and fluorescence increase.[35] The structure of the thymine/Hg^{2+} complex is shown in Figure 1D. Comparing these two designs, the PS-RNA sensor does not require full release of the whole DNA, and thus should be less susceptible to variations in buffer conditions.

Since Hg^{2+} cleaves the PS-RNA linkage very quickly, we also expect faster signaling kinetics. These predictions were tested in the subsequent studies.

DNA probe adsorption. DNA probe adsorption by NGO is the first step of sensor fabrication. For this, we need to choose a good buffer condition. We dissolved Probe 3 (20 nM) in a buffer (50 mM MOP, pH 7.5, 50 mM NaCl, 0.5 mM $MgCl_2$). After scanning the background fluorescence for 8 min, various concentrations of NGO were added and the kinetics of fluorescence drop were monitored (Figure 2). The amount of fluorescence quenching increased with increasing NGO, suggesting more DNA adsorption. Saturated adsorption was achieved with 15 μg/mL of NGO and this concentration was used for the rest of the study.

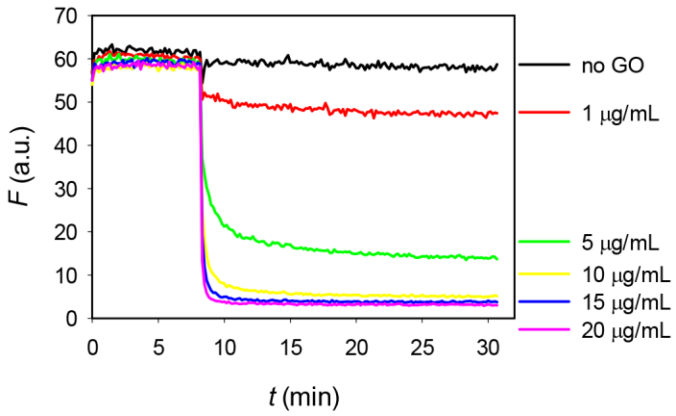

Figure 2. DNA adsorption kinetics with various concentrations of NGO. 20 nM of Probe 3 was used in buffer (50 mM NaCl, 0.5 mM $MgCl_2$, 50 mM MOP, pH 7.5), and NGO was added at the 8 min time point.

Screening for the optimal sequence. After achieving optimal DNA adsorption, we next aim to decide an optimal sequence from the three probes we designed (Figure 1A). First, each probe was incubated with 10 μM Hg^{2+} and then the samples were analyzed by gel electrophoresis

(Figure 3A). We observed a single cleavage band with Probe 1, which contains one PS-RNA modification. Interesting, for the other two probes, in addition to a major cleavage band, a smeared product was also observed. It might be that Hg^{2+} has formed some complexes with the cleaved fragment, which gradually lost the binding interaction during gel electrophoresis. It is clear that more PS-RNA linkages produced more cleavage. In Probe 3 with five PS linkages, nearly 50% of the probe was cleaved.

We then did another assay by adsorbing the DNA probes on NGO followed by adding Hg^{2+} (Figure 3B). As expected, a higher number of the PS RNA linkages gave more signal enhancement, suggesting more cleavage. Therefore, we chose Probe 3 for subsequent studies. Note in this case, we used a relatively high concentration of DNA (250 nM), and the fold of fluorescence increase was quite moderate. For sensor development, the probe concentration was reduced to improve the signal-to-background ratio.

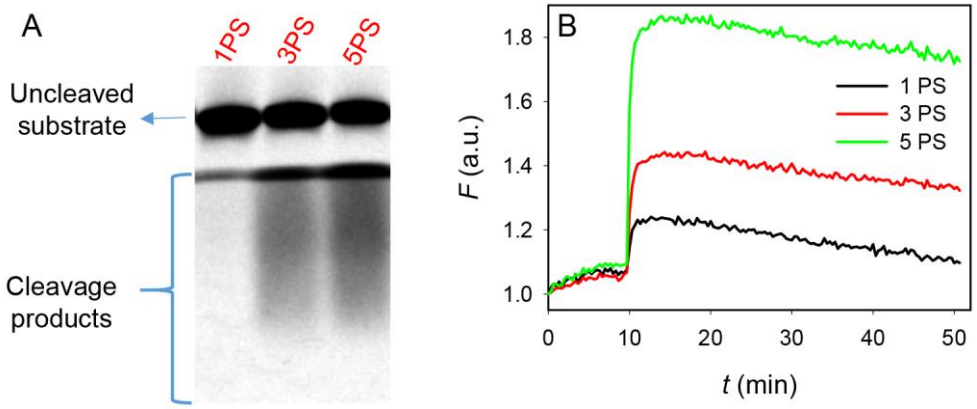

Figure 3. (A) A gel image showing the cleavage products of the three DNA probes incubated with 10 μM Hg^{2+} for 5 min. 1PS, 3PS, 5PS = Probe 1, 2, 3, respectively. (B) Signaling with the three probes after mixing with NGO and then adding 500 nM Hg^{2+} at 10 min.

Sensor performance. Next we tested the sensor response using Probe 3. With increasing concentrations of Hg^{2+}, the signal enhancement was significantly higher (Figure 4A). This experiment confirms the effect of Hg^{2+} as proposed in Figure 1A. The kinetics of fluorescence enhancement is quite fast, reaching saturated signal in ~ 5 min. We then plotted the fluorescence response at 5 min after Hg^{2+} addition (Figure 4B), and a dynamic range to 200 nM Hg^{2+} was obtained. The apparent dissociation constant was 25 nM based on one Hg^{2+} binding. The low Hg^{2+} region response is in the inset of Figure 4B. From it a linear fitting is obtained and the detection limit is calculated to be 8.5 nM Hg^{2+} based on signal higher than three times of background variation. This value is lower than the 10 nM Hg^{2+} defined as the maximal contamination level by the US Environmental Protection Agency (EPA), and thus the sensor might be useful for detecting mercury in water samples.

For the selectivity test, we incubated the sensor with 500 nM of each metal ion and only Hg^{2+} produced strong fluorescence enhancement (Figure 4C). Then the experiment was repeated with a few other metal concentrations. For some environmentally abundant metals, we tested up to 1 mM (Figure 4D). In all the cases, Hg^{2+} produced signal due to its extremely strong thiophilicity. In addition, Tl^{3+} also produced strong signal at 10 μM concentration since it is also a strongly thiophilic metal.[36] Our previous assays indicated that Hg^{2+} can still cleave the PS RNA even in the presence of other metal ions.[24] Overall, using the NGO quencher did not alter the metal interaction trend in this sensing mechanism.

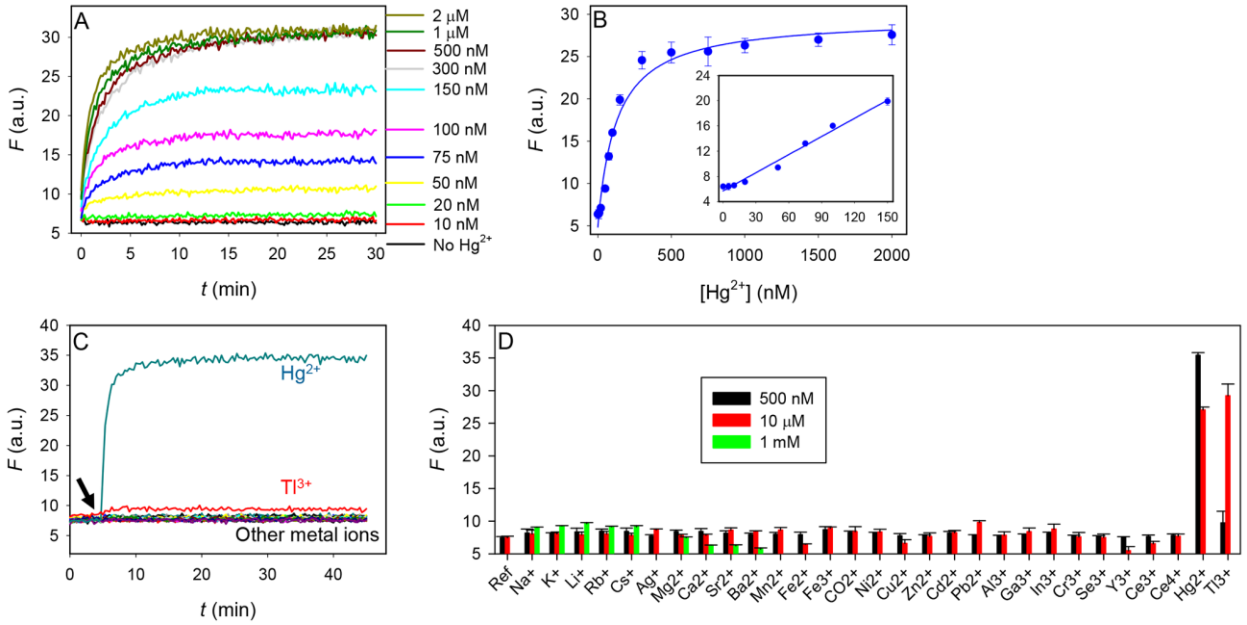

Figure 4. Performance of the PS-RNA based sensor using probe 3. (A) Response of the sensor to various concentrations of Hg^{2+}. (B) Sensor fluorescence signal after 5 min reaction time. Buffer: 50 mM NaCl, 50 mM MOP, pH 7.5, 0.5 mM $MgCl_2$. Inset: response to low concentrations of Hg^{2+}; detection limit = 8.5 nM. (C) Sensor selectivity test with 500 nM of various metal ions. The arrowhead points at the time of metal addition. The tested metal ions are listed in (D). (D) Sensor selectivity at a few metal concentrations.

Comparison with the poly-T probe. Poly-T DNA is the most common method for DNA-based Hg^{2+} detection. Using NGO as the sensing platform, a sensor design is shown in Figure 1C. In this case, this thymine-rich DNA is first adsorbed by NGO, resulting in quenched fluorescence. In the presence of Hg^{2+}, the DNA binds to Hg^{2+} and forms a hairpin structure, desorbing from the NGO surface. This method has already been published previously.[35] Using the same graphene platform gives us an opportunity for a side-by-side comparison.

Since ionic strength and salt type are critical factors for sensor performance, we compared the effect of salt systematically. Both NaCl and $NaNO_3$ were used. In both sensors, the DNA probes were adsorbed by NGO first. When the probes were dispersed in a final of 50 mM $NaNO_3$, we observed comparable fluorescence enhancement for both sensors (Figure 5A), indicating that a similar amount of molecules reacted with Hg^{2+} and produced signal. It is interesting to note though, the PS-RNA-based sensor has a much faster response, where signal stabilized in less than 5 min, while the T-rich DNA still showed signal increase even after 1 h. This is understandable since the Hg^{2+}-induced PS-RNA cleavage takes place quickly, while the thymine-Hg^{2+} binding has to compete with DNA/NGO binding for signal production. A similar observation was made when the $NaNO_3$ concentration was increased to 150 mM (Figure 5B).

When NaCl was used, however, the results were completely different. With 50 mM NaCl (Figure 5C), we still observed a similar amount of fluorescence enhancement with the PS-RNA probe, while the signal increase with the T-rich DNA probe was barely visible. The lack of signal increase cannot be attributed to the ionic strength since the above $NaNO_3$ containing buffer at the same concentration produced much stronger signal increase. Instead this is attributed to complex formation between Hg^{2+} and Cl^-. In other words, Cl^- competes with the DNA for Hg^{2+} binding, leading to a much lower effective Hg^{2+} concentration available to the DNA.[17] This effect is even more pronounced when the NaCl concentration was raised to 150 mM (Figure 5D), where this T-rich DNA probe did not produce any signal increase. By reading the literature on this topic, it is quite easy to notice that most sensors based on the thymine-Hg^{2+} interaction used buffers containing $NaNO_3$ or $NaClO_4$ while avoided high concentrations of NaCl.[11-13] Nitrate and perchlorate are non-coordinating and thus they do not mask Hg^{2+}. However, in real water samples, it is possible that Cl^- is present at a high concentration that may interfere with the

sensing. The reason that Cl^- did not interfere with the PS-RNA sensor is attributable to the much higher affinity between Hg^{2+} and sulfur. This comparison has highlighted an advantage of the sensor design in Figure 1A. It allows higher probe/Hg^{2+} affinity and the sensor is less susceptible to variations in buffer conditions.

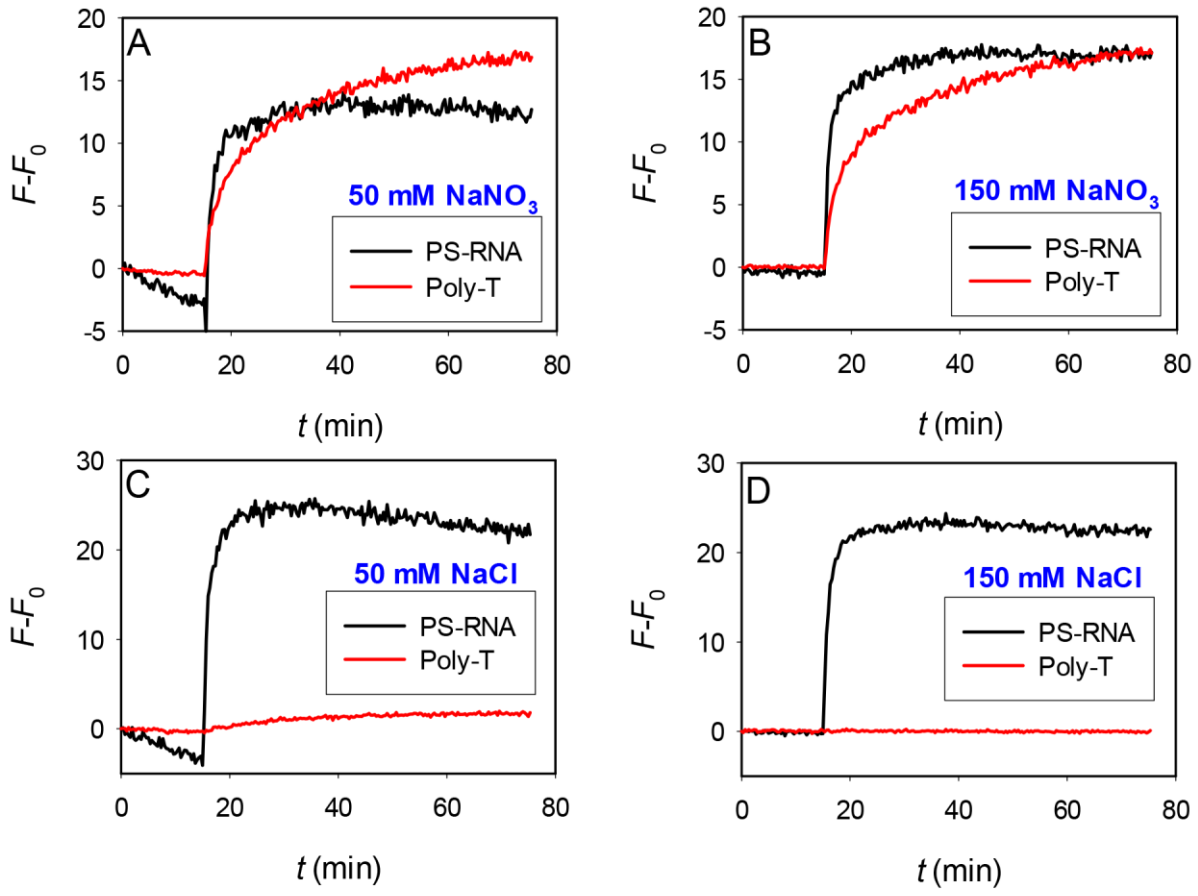

Figure 5. The effect of salt on the performance of the two NGO/DNA-based sensors for Hg^{2+}. The buffer contained (A) 50 mM $NaNO_3$, (B) 150 mM $NaNO_3$, (C) 50 mM NaCl, or (D) 150 mM NaCl. Hg^{2+} was added at 15 min in all the samples.

Conclusions

In summary, we designed a biosensor for Hg^{2+} using DNA containing PS-RNA linkages. Fluorescence quenching is achieved using NGO adsorption. It retains the original selectivity of the PS-RNA chemistry for Hg^{2+}, while eliminating the need for an expensive internal quencher. NGO, the external quencher, produces a detection limit of 8.5 nM Hg^{2+}. In contrast to the commonly used poly-T probe, which responded to Hg^{2+} slowly, a saturated signal enhancement is quickly achieved in less than 5 min for the current sensor. This new sensor is able to function in various buffer conditions, which is more difficult for the T-rich probe. A few advantages of this PS-RNA/NGO sensor can be concluded from this study. 1) GO serves only as a quencher. This allows us to use a block of poly-A DNA for tightly binding to GO. This adsorption function is separated from the Hg^{2+} recognition function using the PS-RNA chemistry. In the poly-T/NGO system, the same DNA is used for adsorption by GO and also for Hg^{2+} binding, making it more susceptible to ionic strength change. Since poly-T DNA is adsorbed less tightly than poly-A DNA, we can envision that the poly-T DNA is more susceptible to non-specific probe displacement as well (e.g. displacement by proteins). 2) The affinity of PS-RNA for Hg^{2+} is stronger than that for the poly-T DNA. Therefore, it is less affected by competing coordinating agents, such as Cl^-. 3) Poly-T DNA has its advantage of being reversible. In the PS-RNA, the detection is based on a chemical reaction and it is difficult to achieve continuous monitoring with it. Taken together, both sensors are highly sensitive and selective for Hg^{2+} detection, and each has its own advantage. The PS-RNA probe might be more useful for testing environmental water samples.

Acknowledgements

Funding for this work is from the Natural Sciences and Engineering Research Council of Canada (NSERC). Grant number: 386326 and STPGP 447472-13.

References

1. A. Renzoni, F. Zino and E. Franchi, *Environ. Res.*, 1998, **77**, 68-72.
2. E. M. Nolan and S. J. Lippard, *Chem. Rev.*, 2008, **108**, 3443-3480.
3. D. W. Domaille, E. L. Que and C. J. Chang, *Nat. Chem. Biol.*, 2008, **4**, 168-175.
4. X.-B. Zhang, R.-M. Kong and Y. Lu, *Annu. Rev. Anal. Chem.*, 2011, **4**, 105-128.
5. J. Liu, Z. Cao and Y. Lu, *Chem. Rev.*, 2009, **109**, 1948–1998.
6. N. K. Navani and Y. Li, *Curr. Opin. Chem. Biol.*, 2006, **10**, 272-281.
7. N. L. Rosi and C. A. Mirkin, *Chem. Rev.*, 2005, **105**, 1547-1562.
8. E. Katz and I. Willner, *Angew. Chem., Int. Ed.*, 2004, **43**, 6042-6108.
9. D. Li, S. P. Song and C. H. Fan, *Acc. Chem. Res.*, 2010, **43**, 631-641.
10. H. Wang, R. H. Yang, L. Yang and W. H. Tan, *ACS Nano*, 2009, **3**, 2451-2460.
11. A. Ono and H. Togashi, *Angew. Chem., Int. Ed.*, 2004, **43**, 4300-4302.
12. J.-S. Lee, M. S. Han and C. A. Mirkin, *Angew. Chem., Int. Ed.*, 2007, **46**, 4093-4096.
13. J. Liu and Y. Lu, *Angew. Chem., Int. Ed.*, 2007, **46**, 7587-7590.
14. X. J. Xue, F. Wang and X. G. Liu, *J. Am. Chem. Soc.*, 2008, **130**, 3244-3245.
15. X. F. Liu, Y. L. Tang, L. H. Wang, J. Zhang, S. P. Song, C. H. Fan and S. Wang, *Adv. Mater.*, 2007, **19**, 1471-1474.
16. M. M. Kiy, Z. E. Jacobi and J. Liu, *Chem. Eur. J*, 2012, **18**, 1202-1208.

17. M. M. Kiy, A. Zaki, A. B. Menhaj, A. Samadi and J. Liu, *Analyst*, 2012, **137**, 3535-3540.

18. P.-J. J. Huang and J. Liu, *Anal. Chem.*, 2014, **86**, 5999-6005.

19. L. A. Cunningham, J. Li and Y. Lu, *J. Am. Chem. Soc.*, 1998, **120**, 4518-4519.

20. M. Hollenstein, C. Hipolito, C. Lam, D. Dietrich and D. M. Perrin, *Angew. Chem., Int. Ed.*, 2008, **47**, 4346 - 4350.

21. R. R. Breaker and G. F. Joyce, *Chem. Biol.*, 1994, **1**, 223-229.

22. J. Liu, A. K. Brown, X. Meng, D. M. Cropek, J. D. Istok, D. B. Watson and Y. Lu, *Proc. Natl. Acad. Sci. U.S.A.*, 2007, **104**, 2056-2061.

23. Z. Liu, S. H. J. Mei, J. D. Brennan and Y. Li, *J. Am. Chem. Soc.*, 2003, **125**, 7539-7545.

24. P.-J. J. Huang, F. Wang and J. Liu, *Anal. Chem.*, 2015, **87**, 6890–6895.

25. C. H. Lu, H. H. Yang, C. L. Zhu, X. Chen and G. N. Chen, *Angew. Chem. Int. Ed.*, 2009, **48**, 4785-4787.

26. Z. Liu, B. Liu, J. Ding and J. Liu, *Anal. Bioanal. Chem.*, 2014, **406**, 6885-6902.

27. D. Chen, H. Feng and J. Li, *Chem. Rev.*, 2012, **112**, 6027-6053.

28. Y. X. Liu, X. C. Dong and P. Chen, *Chem. Soc. Rev.*, 2012, **41**, 2283-2307.

29. Z. W. Tang, H. Wu, J. R. Cort, G. W. Buchko, Y. Y. Zhang, Y. Y. Shao, I. A. Aksay, J. Liu and Y. H. Lin, *Small*, 2010, **6**, 1205-1209.

30. S. J. He, B. Song, D. Li, C. F. Zhu, W. P. Qi, Y. Q. Wen, L. H. Wang, S. P. Song, H. P. Fang and C. H. Fan, *Adv. Funct. Mater.*, 2010, **20**, 453-459.

31. M. Wu, R. Kempaiah, P.-J. J. Huang, V. Maheshwari and J. Liu, *Langmuir*, 2011, **27**, 2731–2738.

32. B. Liu, Z. Sun, X. Zhang and J. Liu, *Anal. Chem.*, 2013, **85**, 7987-7993.

33. L. H. Tang, Y. Wang, Y. Liu and J. H. Li, *ACS Nano*, 2011, **5**, 3817-3822.

34. M. Oivanen, M. Ora, H. Almer, R. Stromberg and H. Lonnberg, *J. Org. Chem.*, 1995, **60**, 5620-5627.

35. X. F. Liu, L. K. Miao, X. Jiang, Y. W. Ma, Q. L. Fan and W. Huang, *Chin. J. Chem.*, 2011, **29**, 1031-1035.

36. P.-J. J. Huang, M. Vazin and J. Liu, *Anal. Chem.*, 2015, **87**, 10443-10449.